RSC Advances

PAPER

View Article Online
View Journal | View Issue

Cite this: *RSC Adv.*, 2014, **4**, 4943

Positive temperature coefficient and structural relaxations in selectively localized MWNTs in PE/PEO blends

Prasanna Kumar S. Mural,[a] Giridhar Madras[a] and Suryasarathi Bose*[b]

The dispersion state of multiwall carbon nanotubes (MWNTs) in melt mixed polyethylene/polyethylene oxide (PE/PEO) blends has been assessed by both surface and volume electrical conductivity measurements and the structural relaxations have been assessed by broadband dielectric spectroscopy. The selective localization of MWNTs in the blends was controlled by the flow characteristics of the components, which led to their localization in the energetically less favored phase (PE). The electrical conductivity and positive temperature co-efficient (PTC) measurements were carried out on hot pressed samples. The neat blends exhibited only a negative temperature coefficient (NTC) effect while the blends with MWNTs exhibited both a PTC and a NTC at the melting temperatures of PE and PEO respectively. These phenomenal changes were corroborated with the different crystalline morphology in the blends. It was deduced that during compression molding, the more viscous PEO phase spreads less in contrast to the less viscous PE phase. This has further resulted in a gradient in morphology as well as the distribution state of the MWNTs in the samples and was supported by scanning electron and scanning acoustic microscopy (SAM) studies and contact angle measurements. SAM from different depths of the samples revealed a gradient in the microstructure in the PE/PEO blends which is contingent upon the flow characteristics of the components. Interestingly, the surface and volume electrical conductivity was different due to the different dispersion state of the MWNTs at the surface and bulk. The observed surface and volume electrical conductivity measurements were corroborated with the evolved morphology during processing. The structural relaxations in both PE and PEO were discerned from broadband dielectric spectroscopy. The segmental dynamics below and above the melting temperature of PEO were significantly different in the presence of MWNTs.

Received 26th September 2013
Accepted 4th November 2013

DOI: 10.1039/c3ra45364b

www.rsc.org/advances

Introduction

Polymer blends have been explored for a wide range of applications due their flexibility in obtaining tailor made properties and are governed by the components, interface and obtained morphologies.[1] The components can either form miscible or immiscible blends depending on the nature of interaction between them. Blending high molecular weight polymers often lead to a small gain in entropy, and hence, most polymer blends are immiscible in nature. However, recent studies have shown that the miscibility can be tuned by incorporating nanoparticles (NPs)[2–4] which can also stabilize the bi-phasic morphology by suppressing droplet coalescence.[5,6]

Selectively localizing conducting particles in any given phase of the blend offers a route to tailor the electrical conductivity by the double percolation phenomenon, first proposed by Sumita *et al.*[7] Due to this selective localization of the conducting particle, the effective concentration increases significantly in the blends.[8–12] Various factors like polarity, rheology, specific interactions and kinetic considerations have been identified, which controls the localization of the NPs in a given phase in the blends. The localization of the NPs can be predicted by thermodynamic consideration provided that the surface free energies of the entities are known. Most often the thermodynamic factors are dominant when the viscosity ratio of both the polymer phases is ~1.[7,13–17] Fenouillot *et al.*[18] reported that viscosity is a major factor for kinetically driven phase morphology. Particles migrate slower when they are confined in the more viscous phase.[16] Kinetic and thermodynamic factors need to be decoupled due to the spatial and localized distribution of particles during mixing.[18]

Conducting polymeric composites find applications in many potential areas like antistatic, electromagnetic interference (EMI) shielding *etc.*[19] Carbon-based composites are attractive due to their flexibility and ease of processing. Among the carbonaceous fillers, carbon nanotubes (CNT) present a high intrinsic conductivity, a high aspect ratio and good mechanical

[a]*Center for Nano Science and Engineering, Indian Institute of Science, Bangalore-560012, India*

[b]*Department of Materials Engineering, Indian Institute of Science, Bangalore-560012, India. E-mail: sbose@materials.iisc.ernet.in*

properties.[20] Recent studies on multiwall carbon nanotubes (MWNTs) have revealed the formation of a conductive path, at a relatively very low content, due to their high aspect ratio, specific surface area and electrical conductivity.[21,22]

Polyolefins are versatile materials used in wide range of potential applications. Although their insulating nature limits their use in the electrical/electronic sectors, the electrical conductivity of polyolefins can be increased by incorporating conducting fillers like CNTs. Studies on a PE nanocomposite with CNTs have demonstrated a higher electrical percolation threshold although, a better filler–filler network is expected in PE due to its nonpolar nature.[20,23,24] On the contrary, the electrical percolation threshold in polar matrices are often observed to be quite high because of strong interaction with the host matrix. The electrical conductivities in the melt (amorphous) and in the semicrystalline matrix can significantly differ due to differences in the dispersion state of the NPs. Although, the selective localization of NPs at the interphase or in one phase reduces the percolation threshold significantly, it is strongly contingent upon the nature of the interactions with the phases.[13,16,17,25,26]

The rationale behind this work is to address the dispersion state of multiwall carbon nanotubes (MWNTs) in PE/PEO blends wherein the flow characteristics of the components differ significantly with respect to the evolved morphology during processing. The energetically favored phase (PEO) has a higher melt viscosity than PE. This further led to the selective localization of the MWNTs in the PE phase and this facilitates the formation of a network like structure of MWNTs at relatively lower concentrations. The evolved morphology during the processing and the subsequent network buildup of the MWNTs in a given phase has been evaluated with respect to both the surface and volume electrical conductivity of the blends. The electrical conductivity measurements, the positive temperature co-efficient (PTC) and the structural relaxations in the blends were analyzed by broadband dielectric spectroscopy. The state of the dispersion of the MWNTs was evaluated using surface and volume electrical conductivity measurements and the morphology was assessed from different depths of the sample by scanning acoustic microscopy.

Experimental section

Materials and methods

Both low density polyethylene (PE with MFI of 25 g per 10 min and density of 0.925 g cm^{-3}) and polyethylene oxide (PEO, M_v = 400 000) were procured from Sigma Aldrich. Multiwall carbon nanotubes (NC 7000) of 90% purity, 9.5 nm diameter and 1.5 μm long were procured from Nanocyl, Belgium. Analytical grades of tetrahydrafuran (THF) and xylene were obtained from commercial sources and were used as received.

70/30 (wt/wt%) PE/PEO blends with and without MWNTs (1–3 wt%) were prepared by melt mixing. Prior to mixing, MWNTs were sonicated in THF using a probe sonicator for 15 min and sonicated (at 25 °C) in a bath for 45 min. Then the solutions were subjected to drying at room temperature followed by in vacuum oven at 80 °C for two days. The PE and MWNTs were dried at 80 °C overnight while PEO was dried at 25 °C in a vacuum oven for 3 h prior to mixing. The neat blends and those with MWNTs were mixed in an intermeshing conical twin screw extruder (Mini Lab II, Haake extruder of 7 mL capacity) using a screw speed of 60 rpm, at 150 °C and for 20 min under a nitrogen atmosphere.

SEM studies support the uniform dispersion of the MWNTs in the blends for the chosen mixing time. A longer mixing time can also result in the thermal degradation of PE and PEO and may destroy the network of the MWNTs.

Characterization

For electrical conductivity measurements, melt mixed strands were molded into discs using a laboratory compression molding machine at 150 °C. The melt viscosities of PE and PEO were measured using a stress controlled rheometer (TA Instruments) with parallel plate geometry at 150 °C. The localization of the MWNTs was studied by a solution experiment (cold water for etching the PEO phase and hot xylene for etching the PE phase). Scanning electron microscopy (SEM) was performed using ULTRA 55, FESEM, Carl Zesis with an accelerating voltage of 5 KV. For the SEM, extruded strands were cryofractured and etched with cold water to remove PEO. Broadband dielectric spectroscopy (in the frequency range of 10^{-1}–10^{7} Hz) was performed on compression molded discs using an Alpha-N Analyzer, Nova Control (Germany) in the frequency range of 0.01–100 KHz and in the temperature range of 35–150 °C with an interval of 5 °C to study the structural relaxations and the bulk electrical conductivity in the blends. *I–V* measurements were performed on compression molded discs using an Agilent Device Analyzer B1500A with pulsed source 5 MHz (van der Pauw four probe technique for surface resistivity and 2 probe for bulk/volume resistivity). The gradient in the morphology was studied using an KSI v400 (Germany) Scanning Acoustic Microscope (SAM) with an operating frequency of 100 MHz in water as an immersion media and the pulse length was 40 ns. The melting temperature (T_m) and crystallization temperature (T_c) were measured using a Mettler Toledo DSC instrument with a heating and cooling rate of 10 K min^{-1}.

Results and discussion

The selective localization of the MWNTs in the PE/PEO blends

The localization of the MWNTs in the 70/30 PE/PEO blends is addressed with respect to the thermodynamic factors and flow characteristics of the components. The wetting coefficient (ω_{12}) can be evaluated, as given in eqn (1), by knowing the surface free energy of the components.

$$\omega_{12} = \frac{\gamma_{P2} - \gamma_{P1}}{\gamma_{12}} \quad (1)$$

γ_{P1}, γ_{P2} and γ_{12} are the interfacial energies between the MWNT (p) and polymer-1, MWNT (p) and polymer-2 and polymer-1 and polymer-2 respectively. If $\omega_{12} > 1$, the particles will preferentially locate in the polymer-1 phase, for $-1 < \omega_{12} < 1$ the particles will reside at the interface and when $\omega_{12} < -1$ the

particles will preferentially locate in the polymer-2 phase. The interfacial tensions are calculated from the surface free energy values.[13,27] Two approaches based on the geometric mean (GM) (eqn (2)) and the harmonic mean (HM) (eqn (3)) can be used to calculate the interfacial tension (γ_{12}) between the polymer–polymer and polymer–particles, respectively.

$$\gamma_{12} = \gamma_1 + \gamma_2 - 4\left(\frac{{\gamma_1}^d{\gamma_2}^d}{{\gamma_1}^d + {\gamma_2}^d} + \frac{{\gamma_1}^p{\gamma_2}^p}{{\gamma_1}^p + {\gamma_2}^p}\right) \quad (2)$$

$$\gamma_{12} = \gamma_1 + \gamma_2 - 2\left(\sqrt{{\gamma_1}^d{\gamma_2}^d} + \sqrt{{\gamma_1}^p{\gamma_2}^p}\right) \quad (3)$$

γ_1, γ_2 are the surface free energies, ${\gamma_1}^d$, ${\gamma_2}^d$ are the disperse part of the surface free energies and ${\gamma_1}^p$, ${\gamma_2}^p$ are polar part of surface free energies of phases 1 and 2 respectively. It is envisaged that the geometric mean is more suitable than the harmonic mean for the polymers with a surface free energy > 20 mJ m^{-1}.[17]

It is important to note that the surface free energy of the polymers is measured from the contact angle measurements taken at room temperature.[28] Surface free energy is temperature dependent and there is no literature for evaluating surface free energy at the processing temperature. Hence, the surface free energy can be calculated at elevated temperatures by extrapolating the values at room temperature using eqn (4) and (5).

$$K = \frac{11}{9}\frac{\gamma_0}{T_c} \times \left(1 - \frac{T}{T_c}\right)^{2/9} \quad (4)$$

$$\gamma = \gamma_0 \times \left(1 - \frac{T}{T_c}\right)^{11/9} \quad (5)$$

In eqn (4), K is the temperature correction factor, γ_0 is the surface free energy at 0 °C, T_c is the critical temperature (For polymers $T_c = 1000$ K) and T is the temperature of the polymer.

Table 1 shows the surface free energy (SFE) and polarities of the polymers and MWNT at 20 °C and 150 °C calculated using eqn (4) and (5). Due to the limited literature about the SFE and the polarity of the MWNTs, a SFE value of 45.6/27.8 mJ m^{-2} and polarity values of 59 and 37% were taken from Nuriel *et al.*[29] and Barber *et al.*[30] Furthermore, the SFE of the MWNTs was taken to be independent of temperature.[17] All other tabulated values were calculated from the existing literature.[28] The interfacial energies calculated for the polymers and the MWNTs are tabulated in Table 1 and it is clearly seen that the PE/PEO blends have a high interfacial energy of 10.02 mJ m^{-2}. Both the harmonic and geometric mean predicted that the MWNTs would be in the PEO phase. However, the MWNTs are observed to be localized in the PE phase and this is strongly contingent upon the flow characteristics of the components. The flow characteristics of the components are studied at the processing temperature *i.e.* 150 °C. It is evident from Fig. 1 that the viscosity of PEO is significantly higher that the PE phase. The higher viscosity of PEO possibly impeded the migration of the MWNTs to the PEO phase during melt mixing.

The gradient in the morphology and dispersion state of the MWNTs

Cryo-fractured surfaces of a 70/30 PE/PEO blend with and without MWNTs are analyzed by SEM. The micrographs obtained are shown in Fig. 2a–f. In order to enhance the phase contrast, the PEO phase is etched out with cold distilled water, as mentioned in the experimental section. Fig. 2 shows that the 70/30 PE/PEO blends exhibit two distinct phases with a matrix-droplet type of morphology. The higher magnification image of Fig. 2c is illustrated in Fig. 2d indicating that the MWNTs are in the PE phase. In order to further support the fact that MWNTs are selectively localized in the PE phase, selective solution dissolution tests were performed (see inset of Fig. 2e). Blend samples with MWNTs are dissolved in the

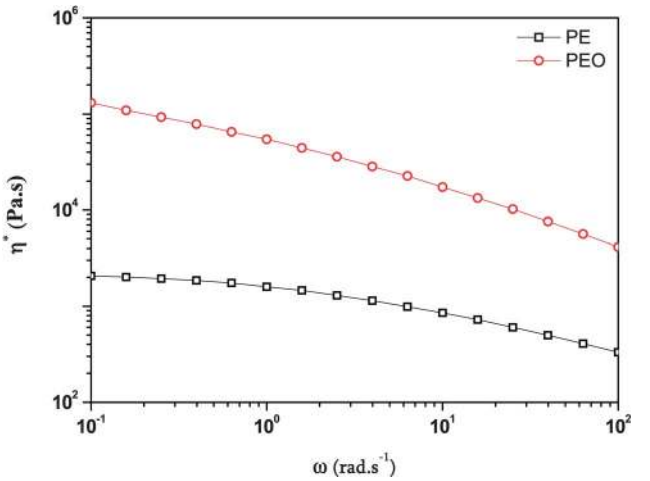

Fig. 1 The flow properties of the components at 150 °C.

Table 1 Thermodynamics parameters for the components as calculated using the harmonic (HM) and geometric mean (GM) equations

	Surface free energy (mN m^{-1})		Polarity (%)		Interfacial energies (mN m^{-1})			Wetting co-efficient ω_A	
	At 20 °C	At 150 °C				HM	GM	HM	GM
PE	35.3	26.8	0	PE/MWNT	Nuriel	28.5	27.7	1.94 (PEO phase)	2.29 (PEO phase)
PEO	42.9	35.9	27.97	PEO/MWNT		9.0	4.7		
MWNT	45.3 (Nuriel[29])	45.3	59.38	PE/PEO		10.0	10.0		
	27.8 (Barber[30])	27.8	37	PE/MWNT	Barber	25.0	21.5	1.60 (PEO phase)	1.70 (PEO phase
				PEO/MWNT		8.9	4.6		

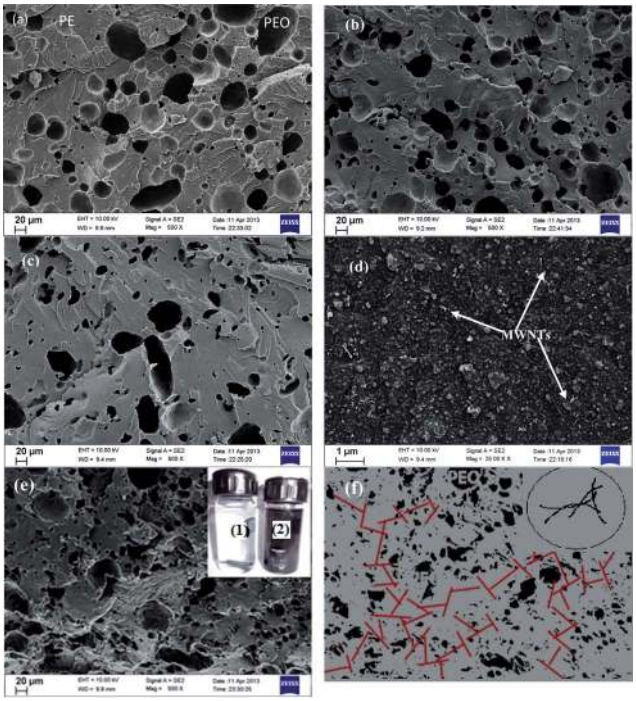

Fig. 2 The cryofractured and etched morphology of 70/30 PE/PEO blends (a) neat (b) with 1 wt% MWNTs, (c) with 2 wt% MWNTs (d) a magnified image of the region indicated (e) with 3 wt% of MWNTs and (f) the possible mechanism of the network formation of the MWNTs (darker regions indicate PEO phase and the brighter regions indicate PE phase). The inset in (e) shows the solution dissolution test; left hand side vial (1) indicates the samples dissolved in cold water to dissolve the PEO phase and the vial on the right hand side indicates the sample dissolved in hot xylene to dissolve the PE phase.

respective solvent (cold water for PEO and hot xylene for PE). It is found that the clear hot xylene solution turned black in color when the PE phase is completely dissolved suggesting that the MWNTs are suspended in the xylene solution. However, no observable change is noticed in the blend samples dissolved in cold water. Thus, it is evident that the MWNTs are selectively localized in the PE phase. Li *et al.*[31] showed that in carbon black (CB) filled PP/ultra high molecular weight poly(ethylene) (UHMWPE) blends, the CB were localized mostly in the PP phase (thermodynamically less favored phase) rather than in the UHMWPE phase. They suggested that the CB particles were not able to migrate to the energetically favored phase (UHMWPE) due to the high viscosity of UHMWPE in contrast to PP.

Although the PEO phase is energetically more favored, the localization of the MWNTs here is governed by the flow characteristics of the components. It is generally agreed that the MWNTs are randomly distributed and dispersed in the amorphous region of PE due to the volume exclusion effect. Random distribution and dispersion leads to an increase in the effective filler concentration[8,12] and the interconnected network structures in the MWNTs. Thus, the interconnected networks increase the conductivity, which is consistent with the dielectric studies and will be discussed in more detail in the subsequent sections.

The selective localization of the MWNTs in the PE phase forms a 3D network structure above the percolation threshold.[32] This promotes the electrical conductivity in the blends by providing the conductive pathway for electrons to tunnel. Since MWNTs are selectively localized in the PE phase, the non-polar nature of PE will facilitate in better filler–filler network lowering the percolation threshold. The cartoon in Fig. 2f shows the possible mechanism of the MWNT network formation in the PE phase in the blends.

Bulk and surface electrical conductivity in PE/PEO blends

Fig. 3 shows the frequency dependence of the AC electrical conductivity of the 70/30 PE/PEO blends with varying concentrations of MWNTs at room temperature. The bulk electrical conductivity of the 70/30 PE/PEO blends with the MWNTs increases with the increasing concentration of the MWNTs. With the addition of 1 wt% MWNTs, a jump in the conductivity of 3 orders of magnitude is observed while with the addition of 2 and 3 wt% of MWNTs, an increase of 7 orders (*i.e.* from $\sim 10^{-13}$ to $\sim 10^{-6}$ S cm^{-1}) is noted manifesting that the percolation threshold in the 70/30 PE/PEO blends is between 1 and 2 wt%. Table 2 shows the variation of σ_{dc} as a function of the MWNT concentration obtained by fitting the AC conductivity plots with the scaling law (see eqn (6)). An abrupt increase in the conductivity is observed for the 70/30 PE/PEO blends at 2 wt% loading of MWNTs and the AC conductivity exhibits a frequency independent plateau over a wide range of frequency. The possible reason for this behavior could be attributed to the formation of a network like structure of MWNTs, as shown in the cartoon presented in Fig. 2f. It is important to note that earlier reports indicate a relatively higher percolation threshold of 3.6 vol% (~6 wt%) in PE/MWNT composites.[24,33] Naguib *et al.*[24] found a DC conductivity of the order of 2.03×10^{-7} S cm^{-1} for 5 wt% MWNTs in PE. The percolation threshold in this study is between 1 and 2 wt% MWNTs indicating a relatively better dispersion state of the MWNTs in the PE phase. Based on

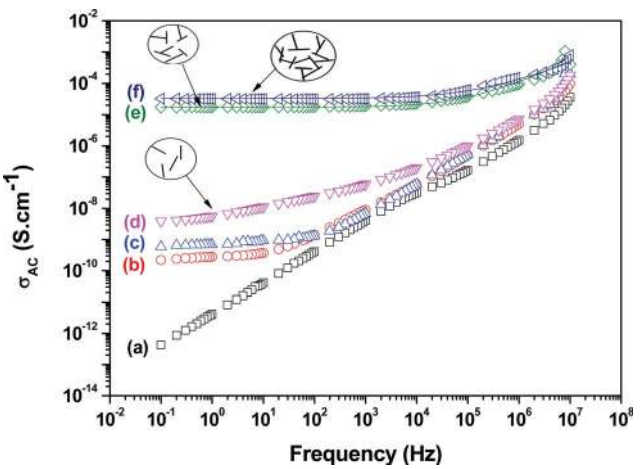

Fig. 3 The dielectric conductivity of (a) PE (b) PEO (c) neat blends (d) with 1 wt% (e) with 2 wt% and (f) with 3 wt% MWNTs (the continuous solid line indicates the scaling law fitted line and the cartoons indicate the mechanism of the network formation of the MWNTs).

Table 2 The surface and volume electrical conductivity of various blends

	σ_{dc} (S cm^{-1})	f_c (Hz)	s	Surface conductivity using four probe (S cm^{-1})	Volume conductivity using two probe (S cm^{-1})
PE	4.2×10^{-13}	—	1.06	—	—
PEO	2.2×10^{-10}	11	1.03	—	—
70/30 PE/PEO	5.9×10^{-10}	97	1.07	1.5×10^{-13}	—
70/30 PE/PEO blend with 1 wt% MWNT	3.9×10^{-9}	1.4×10^{3}	1.03	7.7×10^{-4}	7.3×10^{-11}
with 2 wt% MWNT	1.7×10^{-6}	1.4×10^{5}	0.71	1.4×10^{-3}	4.7×10^{-5}
and with 3 wt% MWNT	3.3×10^{-6}	1.6×10^{5}	0.61	2.7×10^{-3}	9.7×10^{-5}

this, one can argue that the double percolation is achieved at a much reduced concentration.[34] One more argument that can address the relatively lower percolation threshold of the MWNTs in LDPE is a lower crystallinity as compared to HDPE and LLDPE where the percolation threshold of the conducting filler is relatively higher. A further analysis of the frequency dependence of the AC conductivity at room temperature was done using a power law behavior[35] with eqn (6).

$$\sigma'(\omega) = \sigma(0) + \sigma_{ac}(\omega) = \sigma_{dc} + A\omega^{s} \quad (6)$$

where, ω is the angular frequency, σ_{dc} is the direct current (DC) conductivity, A is the temperature dependent constant and s is the exponent dependent on both frequency and temperature with value ranging from 0–1.

From Fig. 3, σ_{dc} was estimated by fitting the conductivity response of the nanocomposite. Due to the difference in the permittivity and the conductivity between the blends and the MWNTs there will be an accumulation of charge carriers at the interface resulting in space charge polarization.[35] Table 2 tabulates the various parameters of the PE/PEO blend nanocomposite DC conductivity (σ_{dc}), crossover frequency (f_c), and exponent 's' for the samples. σ_{dc} and f_c increase with the incorporation of the MWNTs. The value of 's' decreases from 1 to 0.7 with an increase in the MWNT concentration from 1 to 2 wt%, which infers the formation of 3D networks of capacitors.[35] Furthermore, this corresponds to a 30% capacitance and 70% resistance equivalent network.[36] Similarly, for 3 wt% of MWNT loading, $s = 0.6$ indicating the formation of 3D networks with a resistance to capacitance ratio of 60 : 40 in the blends.

Fig. 4 shows the I–V characteristic of the 70/30 blends with 1–3 wt% MWNTs. It is evident that the contact of the MWNTs is ohmic in nature in the blends. It can be inferred that there is the formation of a MWNT network and electrons can tunnel. Similar plots were obtained for 1 wt% MWNTs for both across the thickness and on the surface of the sample. But for 70/30 neat, an obvious non ohmic characteristic was observed. Furthermore, van der Pauw measurements for the surface analysis (2D) and two probe measurements across the thickness (3D) were performed. The surface conductivity was observed to be higher by 2 orders in magnitude in contrast to the conductivity across the thickness. This could be attributed to the gradient in the morphology as will be discussed later on. Presumably, during compression molding, the less viscous PE ($\eta_{PE} = 2027$ Pa s) phase spreads more on the surface, while the higher viscous PEO spreads less during molding. This leads to a gradient in the morphology of the sample and PEO spreads only at the center of the sample. This possibly could be one of the reasons behind the different surface and volume conductivities in the PE/PEO blends. In order to confirm this hypothesis, SAM and contact angle measurements are performed on the compression molded specimens.

SAM images are taken by etching out the PEO phase. Fig. 5 shows that there is a gradient of PEO (dark) on the surface; mostly segregated at the center, whereas at a depth of around 170 μm, there is a uniform distribution of the PEO (dark) and PE phases (bright). Thus, the gradient in morphology could possibly lead to a higher conductivity on the surface than across the thickness. A higher conductivity further confirmed that the MWNTs are selectively localized in the PE phase. In order to reconfirm, SEM was done on the compression molded discs. The SEM micrographs (Fig. 6) further confirmed the presence of PE rich phases on the surface and a gradient in the morphology across the thickness in the cryofractured and etched (to remove the PEO phase) surfaces. The contact angle at the edge of sample is *ca.* 94° and at the center it is *ca.* 62° which further confirms the presence of PEO only at the center of the sample. The higher contact angle at the edge essentially suggest a PE phase and the relatively lower contact angle at the edge possibly indicates the segregation of the PEO phases only at the center of the specimens.

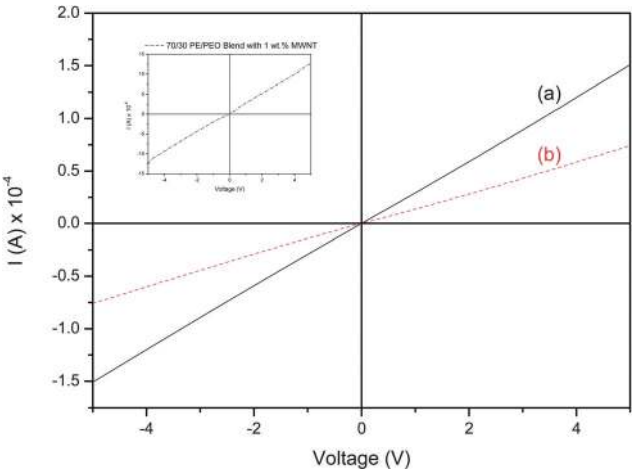

Fig. 4 The I–V measurements of the 70/30 PE/PEO blend (a) with 2 wt% and (b) with 3 wt% MWNTs (the inset shows the I–V measurements of the 70/30 PE/PEO blend with 1 wt% MWNTs).

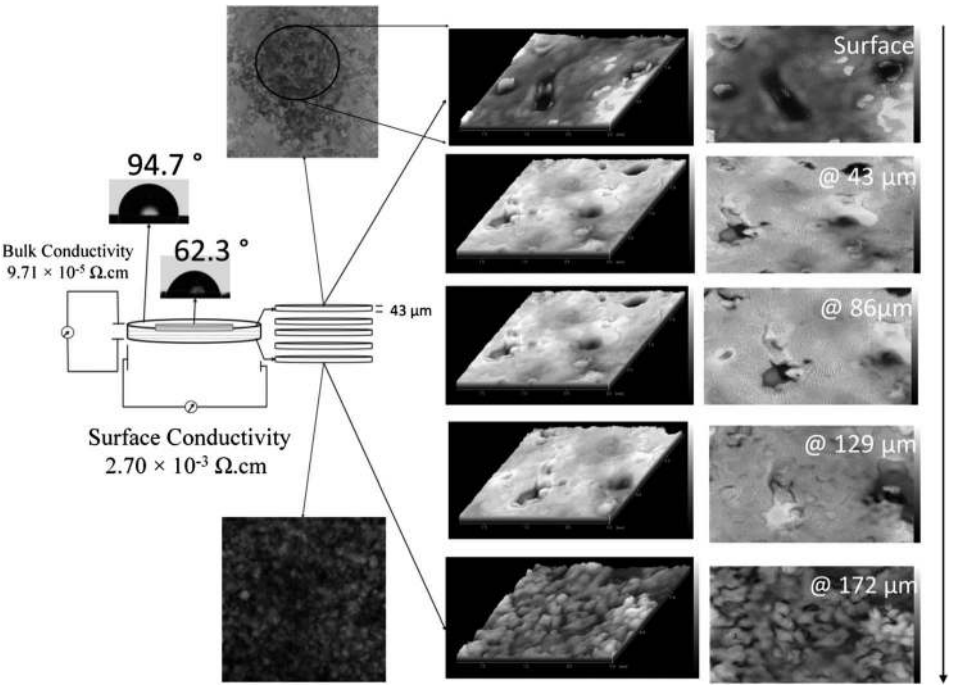

Fig. 5 Scanning acoustic microscope (SAM) images of the 70/30 PE/PEO blend with 3 wt% MWNTs of which PEO is etched out. Images from various depths are shown here (the brighter regions are the PE phase and the darker regions are the PEO phase) (the contact angle is also shown here).

NTC and PTC effects in PE/PEO blends

It is evident from the above analysis that beyond a critical concentration of MWNTs, a continuous conducting path (percolation threshold) is formed in the PE phase of the blends.[37,38] The increase in the conductive network results in a reduction of the gap between adjacent CNTs to few nanometers (≤10 nm, equivalent to physical contact[9]). The physical contact of the MWNTs provides a network path for the easy hopping of electrons and thus conductivity is induced in the PE/PEO blends. The effect of the DC conductivity as a function of temperature in the range of 35 °C–150 °C at a particular frequency is studied on PE/PEO blends for both the neat blend and in the presence of MWNTs. The variation of the DC conductivity with temperature for PE/PEO (70/30) filled with 1–3 wt% of MWNTs is shown in Fig. 7a–d.

The positive temperature co-efficient (PTC) refers to materials that exhibit a sharp decrease in the electrical conductivity upon heating in the vicinity of the melting region of a semi-crystalline matrix. Fig. 4 shows the DC conductivity as a function of temperature and the DSC thermograms for respective PE/PEO (70/30) blends with MWNTs are incorporated in the same figure for a clear comparison. For neat blends, the conductivity increases sharply around 60 °C and moderately rises beyond this temperature indicating a negative temperature coefficient effect. The increase in the conductivity around 60 °C could be due to the melting of the PEO phase, as shown in Fig. 7a. The amorphous regions in PEO promote the ionic mobility above the melting point of PEO.[39] In the case of PEO, the influence of the lamellar crystallites plays an important role and reduces the conductivity substantially. Thus, at the melting temperature of PEO we observe a transition from long-range conductivity (above T_m) to a more localized ionic motion (below T_m) within the amorphous regions.

For the PE/PEO (70/30) blends with 1–3 wt% of MWNTs, a slight increase in the conductivity at 60 °C followed by a decrease in conductivity is observed at 100 °C, which coincides with the onset of the melting point of PE as observed from the DSC melting endotherm. Furthermore, a decrease in conductivity is observed indicating a positive temperature coefficient (PTC) effect in the blend. At 115 °C, the decrease in the conductivity is saturated. A further increase in the temperature *i.e.*, from 120 to 150 °C leads to an increase in conductivity. When the temperature attains the melting point (T_m) of PE, PE starts to melt which results in volume expansion leading to disruption in the conductive networks of the MWNTs. As a result of this, a decrease in conductivity is observed leading to a PTC effect.[40] Different mechanisms have been proposed to explain this effect. For instance, Li *et al.*,[31] suggested that the decrease in conductivity at T_m is also observed for poly(propylene) (PP)/ultra high molecular weight poly(ethylene) (UHMWPE) filled with carbon black (CB). They observed that CB particles are rejected from the growing crystalline fronts during crystallization. Thus, the CB particles are dispersed homogenously in the amorphous region forming a network. When the crystallites melt, CB particles disperse into the polymer melt resulting in an increase in the inter particle distance. The increase in the inter particle distance impedes the electron tunneling between conductive particles thus resulting in the decrease in conductivity. Rahaman *et al.*,[37] suggested that in EVA/NBR blends, above T_m, ethyl vinyl acetate (EVA) gets softer

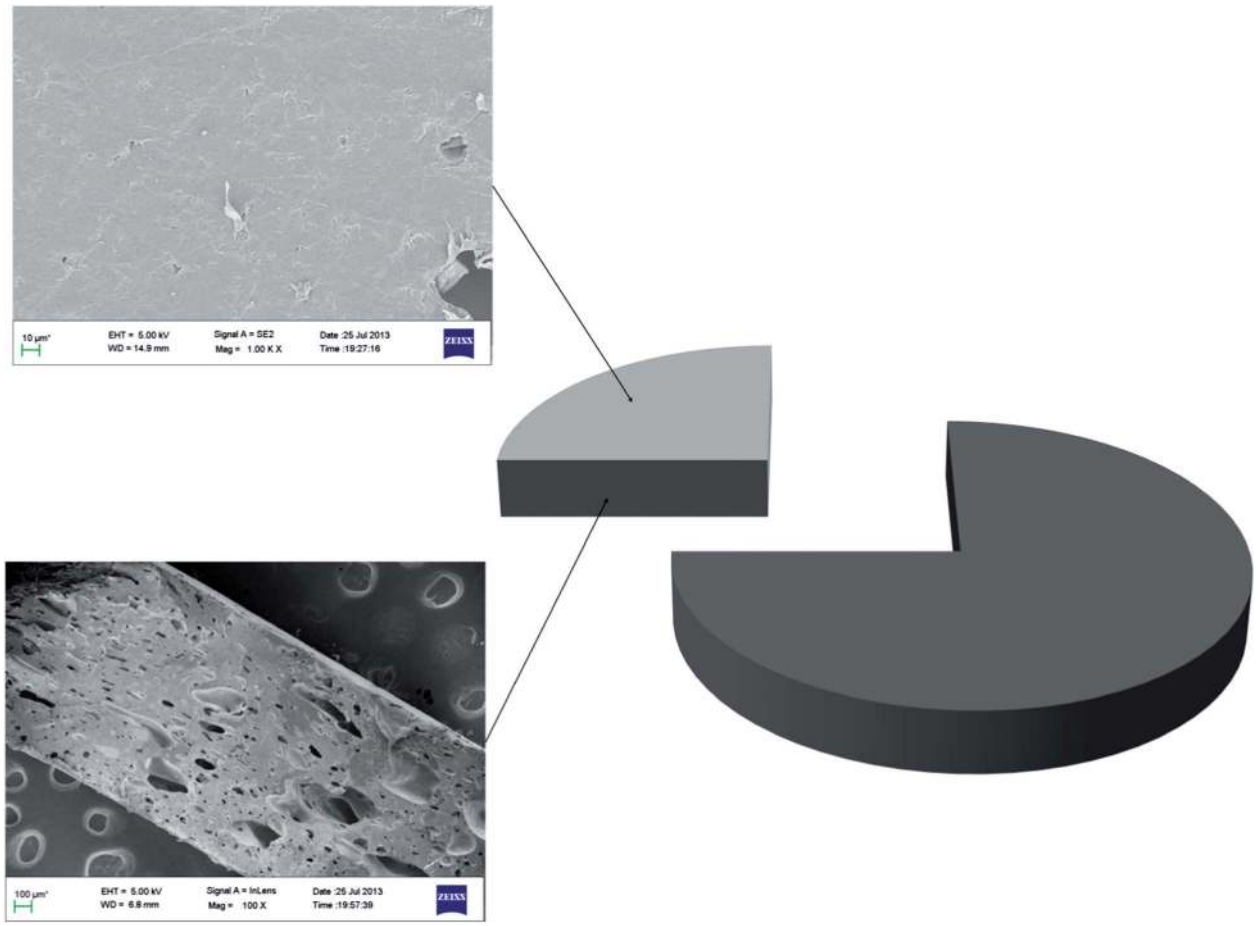

Fig. 6 SEM micrographs of the 70/30 PE/PEO blend with 3 wt% MWNTs.

and thus reduces polymer viscosity. The reduction in viscosity led to the thermal agitation of the polymer chains resulting in aggregation of the fillers and hence a higher conductivity.

With a further increase in the temperature, an increase in the conductivity is observed, which could be attributed to a decrease in the polymer viscosity which results in the Brownian motion of the chains that progressively leads to the rearrangement of the MWNT conductive network. Thus, a sharp increase in conductivity is observed.[37] It is evident that the PEO phase present in the 70/30 PE/PEO blend does not have any effect on the PTC behavior. Furthermore, at the T_m of PE, the PTC is exhibited supporting the fact that the MWNTs are localized selectively in the PE phase, which is consistent with the results obtained from the SEM and solution dissolution experiments.

The permittivity (ε') of the blends with and without MWNTs (1 wt%) is shown in Fig. 8. It is envisaged that the dielectric permittivity increases because of the charges trapped at the crystal–amorphous interface and also at the interface of dissimilar materials (dielectric *versus* conducting particles). The increase in ε' is more evident than the DC conductivity (in Fig. 7) due to the above mentioned fact. The ε' abruptly decreases as the PEO crystals start melting due to the loss of interface within the PEO. A similar trend is noted as the PE crystals start melting however, beyond the melting temperature of PE the ε' rises sharply due to charges trapped at the interfaces of the polymer chains and the MWNTs. The Brownian motion of the former increases with an increase in the temperature and facilitates random network of MWNTs at a higher temperature. Similar observations are noted at 2 and 3 wt% MWNTs. These observations are strikingly different from the control blends shown as the inset in Fig. 8. Here, the ε' rises sharply both at the melting temperature of PEO and PE which is very similar to the DC conductivity. It is apparent that the charges trapped at the crystal–amorphous interface are less pronounced in comparison to the charges trapped at the dissimilar materials (conducting *versus* dielectric) which explains the ε' behavior in the blends.

A schematic representation is shown in Fig. 9 which clearly demonstrates the various effects as a function of temperature. Below the melting temperature of PEO, the lamellar crystallites decrease the overall conductivity in PEO as they restrict the ionic mobility in the amorphous regions. However, at the melting temperature of PEO, an abrupt increase in the conductivity suggests an NTC effect where the long range ionic mobility is facilitated. As the MWNTs are selectively localized in the PE phase, a strong PTC effect is noted suggesting an impeded conduction pathway of the MWNTs due to the volume expansion at the melting temperature of PE. At temperatures

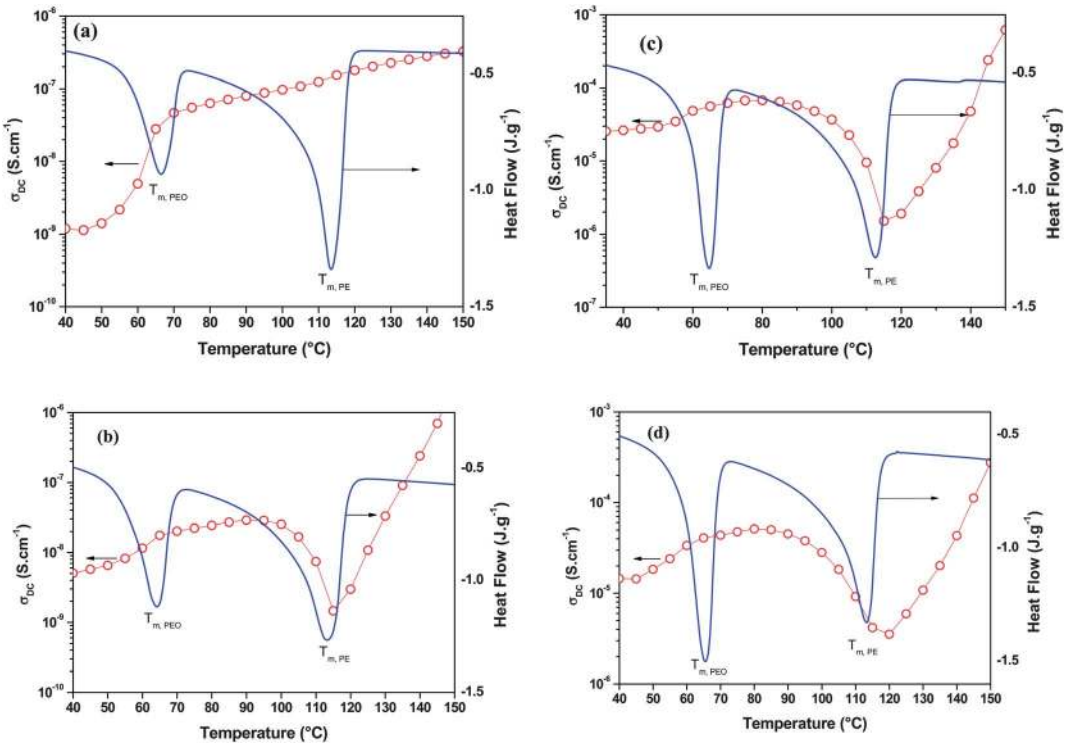

Fig. 7 The dielectric conductivity (at 1 Hz) as a function of temperature for (a) the 70/30 PE/PEO neat blends, (b) the blends with 1 wt% MWNTs, (c) the blends with 2 wt% of MWNTs, and (d) with 3 wt% MWNTs along with the corresponding DSC thermograms.

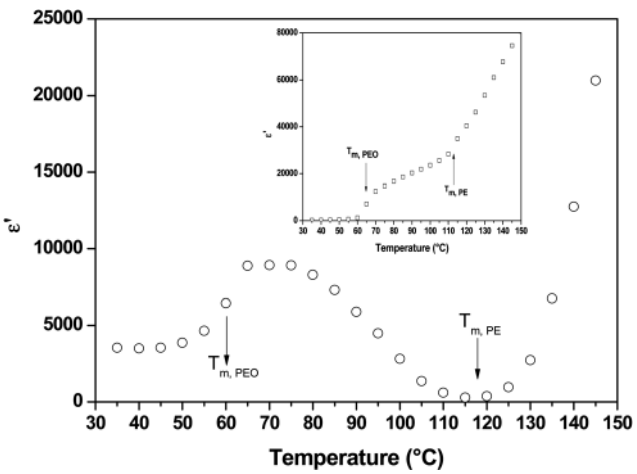

Fig. 8 The dielectric constant at various temperatures for the 70/30 PE/PEO blend with 1 wt% MWNTs (the inset shows permittivity as a function of temperature for the 70/30 PE/PEO neat blends).

above the melting temperature of PE and PEO, the conductivity rises significantly owing to the ionic mobility in the amorphous regions in the case of PEO and the random network buildup of the MWNTs at higher temperatures in the PE phase.

Structural relaxations in PE/PEO blends in presence of MWNTs

It is envisaged that the conductivity behavior in PEO is significantly different, due to its slow crystallization, above and below the melting temperature. Hence, the change in the crystalline morphology significantly affects the conduction mechanism in PEO. The relaxations in PEO mainly arise from the polymer motions in the regions between the amorphous and crystalline phases termed as interphase.

Fig. 10 shows the dielectric loss modulus loss spectra (M'') as a function of frequency for various compositions investigated here. It is interesting to note that neat PEO shows two distinct relaxations presumably arising from the conductivity relaxations at lower frequencies and structural relaxations at higher frequencies (as indicated in Fig. 10). The latter has been assigned based on the observation that this particular relaxation is observed to shift towards higher frequencies with an increase in temperature (not shown here). On the other hand, neat PE shows only one relaxation at a higher frequency (shown as inset in Fig. 10). Interestingly, the neat 70/30 PE/PEO blends exhibit a distinct peak in the lower frequency side suggesting structural relaxation in PEO. This particular relaxation appears at a much lower frequency than the neat PEO suggesting a slowing of the structural relaxations upon blending. The relaxations associated with PE are very well discerned from the high frequency shoulder (as indicated in Fig. 10). It is evident from the conductivity measurements that neat PEO and the 70/30 PE/PEO blends show almost similar DC conductivities below the melting temperature of PEO which essentially suggests that the ionic mobility in the amorphous segments of PEO is unaltered below the melting temperature of PEO in the blends. However, these effects significantly vary above the melting temperature of PEO and will be discussed in detail subsequently.

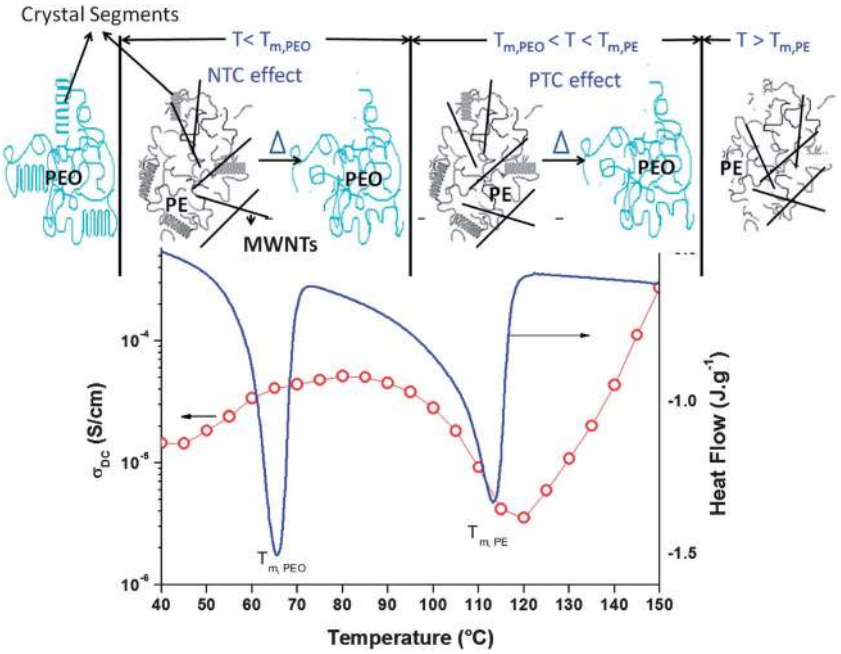

Fig. 9 A schematic representation of the NTC and PTC effect exhibited by the 70/30 PE/PEO blend with MWNTs at temperatures below and above the melting temperature of PEO and PE. (The solid lines in the PE phase represent the MWNTs.)

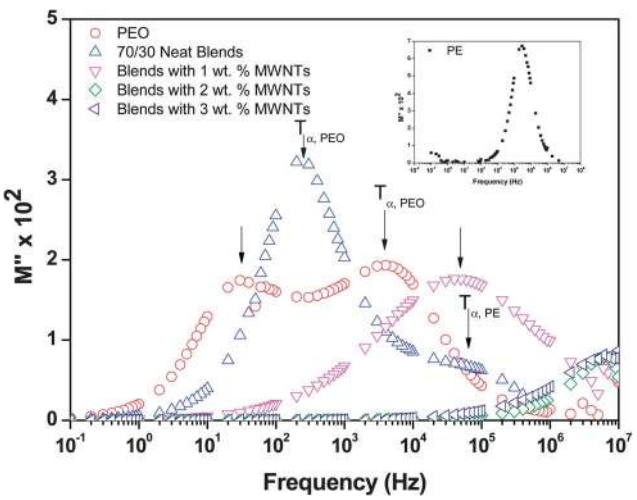

Fig. 10 The dielectric loss modulus as a function of frequency for PEO, the 70/30 blends with and without MWNTs at 40 °C (inset shows dielectric loss modulus of neat PE at 40 °C).

Interestingly, the blends with 1 wt% MWNTs only show a single broad relaxation spectrum at a higher frequency and we could hardly capture the relaxations for blends with a higher fraction of MWNTs in the measured frequency window (10^{-1}–10^{7} Hz). Hence, in the subsequent discussion we will discuss only blends with 1 wt% MWNTs and compare the spectra with respect to the neat blends. The flat relaxation behavior in the blends with 1 wt% MWNTs suggests that the low frequency relaxations are not resolved in the spectra. The broadness of the peak on the high frequency side below the melting temperature of both PEO and PE suggest the faster segmental polymer dynamics of PEO due to the geometrical constraints from the interface formed by the crystalline spherulites. The DSC measurements shown in Table 3 further confirm that there is a slight decrease in the % crystallinity of the neat PE and an increase in the % crystallinity of the neat PEO on blending and the addition of MWNTs. But the melting temperatures of PE and PEO are almost unaffected, suggesting the formation of lamellae in both the neat blend and the blends filled with 1–3 wt % MWNTs. Hence, the formation of lamellar crystallites gives rise to interphase regions and exhibit a faster segmental relaxation than the amorphous regions of the polymer. It is worth recalling that the MWNTs are selectively localized in the PE phase of the blends. Hence, the segmental dynamics of PE are expected to be significantly affected by MWNTs. However, due to geometrical constrains it appears that both the conductivity and the structural relaxations of PEO are also significantly affected due to the PE phase filled with MWNTs.

The relaxation spectra for the neat 70/30 blend and blends with 1 wt% MWNTs are shown in Fig. 11 in the temperature range of our interest (40–140 °C). It is interesting to note that below the melting temperature of PEO, the polymer may consist of lamellar crystals, amorphous regions, and interphase. The formation of the crystalline regions severely restricts the long-range ionic mobility by disrupting the conduction pathways in the amorphous regions. This is evident by the abrupt enhancement of the conductivity above the melting temperature of the crystalline regions (see discussion related to NTC effect). From the M'' *versus* frequency curves, it is evident that the structural relaxation of PEO is observed to shift towards higher frequencies with an increase in temperature. The higher frequency shoulder pertaining to PE relaxations also shifts towards a higher frequency and could not be captured beyond a

Table 3 The crystallization and melting parameters of the PE/PEO blends with and without MWNTs

	Melting temperature T_m (°C)		Crystalline temperature T_c (°C)		% Crystallinity	
	PE	PEO	PE	PEO	PE	PEO
70/30 PE/PEO blends	111.7	63.1	100.4	44.8	27.3	9.6
70/30 PE/PEO blends with 1 wt% MWNTs	113.4	64.6	99.4	43.8	25.5	13.7
with 2 wt% MWNTs	112.2	65.2	100.5	41.8	24.6	17.4
with 3 wt% MWNTs	113.7	65.8	100.7	44.0	23.2	19.9

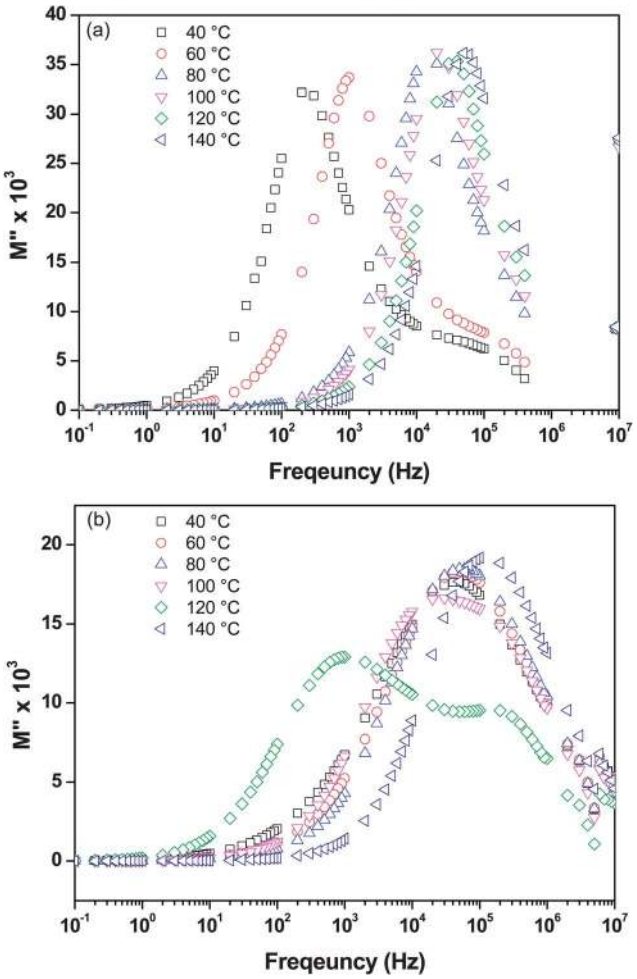

Fig. 11 The dielectric modulus loss *vs.* frequency at various temperatures of (a) the 70/30 neat blend (b) with 1 wt% MWNTs.

certain temperature due to the limited frequency range. Interestingly, for the blends with 1 wt% MWNTs, beyond the melting temperature of PEO and at the onset of PE melting, two distinct peaks can be observed. The low frequency peak can be assigned to the conductivity relaxation of PEO which also showed an abrupt rise above the melting temperature of PEO. More interestingly, beyond the melting temperature of PE the peak at a lower frequency completely disappears and a single broad relaxation appears, which is a characteristic of amorphous relaxation. Thus, at the melting temperature of PEO, we observe a transition from long-range conductivity (above T_m) to a more localized ionic motion (below T_m) within the amorphous regions and hence, the structural (α) relaxation process is caused by more localized segmental dynamics.

Conclusions

The dispersion state of the multiwall carbon nanotubes (MWNTs) in melt mixed polyethylene/polyethylene oxide (PE/PEO) blends was assessed by both surface and volume electrical conductivity measurements. The flow characteristics of the components govern the selective localization of the MWNTs in the blends, which led to their localization in the thermodynamically less favored phase (PE). PE/PEO blend exhibited a matrix droplet morphology. The electrical conductivity of the PE/PEO blend increased by 7 orders of magnitude in the presence of 2 wt% MWNTs. The *I–V* measurements indicated differences of 2 orders of magnitude across the surface and the bulk conductivity. Both the NTC and PTC effect was observed in the 70/30 PE/PEO blends at the melting temperature of PEO and PE respectively. The compression molded samples exhibit a gradient in the microstructure in the PE/PEO blends, which was assessed by SAM at different depths and further confirmed by measuring the contact angle at various locations. The neat 70/30 PE/PEO blends exhibited a distinct relaxation peak in the lower frequency side concerning the structural relaxation in PEO. From the M'' *versus* frequency curves, it is evident that the structural relaxation is observed to shift towards higher frequencies with an increase in the temperature. The relaxations speed-up due to geometrical constraints from the interface formed by the crystalline spherulites. At the melting temperature of PEO, we observe a transition from the long-range conductivity (above T_m) to a more localized motion (below T_m) within the amorphous regions. Beyond the melting temperature of PE, the peak at the lower frequency completely disappeared and a single broad relaxation appears, which is a characteristic of amorphous relaxation.

Acknowledgements

Department of Science and Technology (DSTO1150) and JATPO 0136 is gratefully acknowledged for the financial support. We would like to thank MNCF, CeNSE for providing instrumentation facilities.

References

1 L. A. Utracki, *Polymer Blends Handbook*, Kluwer Academic Pub, 2002.
2 P. Xavier and S. Bose, Multiwalled-Carbon-Nanotube-Induced Miscibility in Near-Critical PS/PVME Blends: Assessment through Concentration Fluctuations and Segmental Relaxation, *J. Phys. Chem. B*, 2013, **117**(28), 8633–8646.
3 K. Sharma, M. Sharma, A. Chandra and S. Bose, Concentration Fluctuations and Segmental Dynamics in Weakly Dynamic Asymmetric Blends in the Presence of Surface-Functionalized Multiwall Carbon Nanotubes, *Macromol. Chem. Phys.*, 2013.
4 M. Sharma, K. Sharma and S. Bose, Segmental Relaxations and Crystallization-Induced Phase Separation in PVDF/PMMA Blends in the Presence of Surface-Functionalized Multiwall Carbon Nanotubes, *J. Phys. Chem. B*, 2013, **117**(28), 8589–8602.
5 S. Bose, A. R. Bhattacharyya, P. V. Kodgire, A. Misra and P. Pötschke, Rheology, morphology, and crystallization behavior of melt-mixed blends of polyamide6 and acrylonitrile-butadiene-styrene: Influence of reactive compatibilizer premixed with multiwall carbon nanotubes, *J. Appl. Polym. Sci.*, 2007, **106**(5), 3394–3408.
6 S. Bose, C. Ozdilek, J. Leys, J. W. Seo, M. Wubbenhorst, J. Vermant and P. Moldenaers, Phase separation as a tool to control dispersion of multiwall carbon nanotubes in polymeric blends, *ACS Appl. Mater. Interfaces*, 2010, **2**(3), 800–807.
7 M. Sumita, K. Sakata, S. Asai, K. Miyasaka and H. Nakagawa, Dispersion of fillers and the electrical conductivity of polymer blends filled with carbon black, *Polym. Bull.*, 1991, **25**(2), 265–271.
8 H.-D. Bao, Z.-X. Guo and J. Yu, Effect of electrically inert particulate filler on electrical resistivity of polymer/multi-walled carbon nanotube composites, *Polymer*, 2008, **49**(17), 3826–3831.
9 S. K. Bose, A. Rupesh and P. Moldenaers, Assessing the strengths and weaknesses of various types of pre-treatments of carbon nanotubes on the properties of polymer/carbon nanotubes composites: A critical review, *Polymer*, 2010, **51**(5), 975–993.
10 N. F. Colaneri and L. W. Schacklette, EMI shielding measurements of conductive polymer blends, Instrumentation and Measurement, *IEEE Trans. Instrum. Meas.*, 1992, **41**(2), 291–297.
11 W. Thongruang, C. M. Balik and R. J. Spontak, Volume-exclusion effects in polyethylene blends filled with carbon black, graphite, or carbon fiber, *J. Polym. Sci., Part B: Polym. Phys.*, 2002, **40**(10), 1013–1025.
12 X. Yang, S. Shang and L. Li, Layer-structured poly(vinyl alcohol)/graphene oxide nanocomposites with improved thermal and mechanical properties, *J. Appl. Polym. Sci.*, 2011, **120**(3), 1355–1360.
13 R. Cardinaud and T. McNally, Localization of MWCNTs in PET/LDPE blends, *Eur. Polym. J.*, 2013, **49**(6), 1287–1297.
14 J. Feng, C.-m. Chan and J.-x. Li, A method to control the dispersion of carbon black in an immiscible polymer blend, *Polym. Eng. Sci.*, 2003, **43**(5), 1058–1063.
15 A. Göldel, A. Marmur, G. R. Kasaliwal, P. Pötschke and G. Heinrich, Shape-Dependent Localization of Carbon Nanotubes and Carbon Black in an Immiscible Polymer Blend during Melt Mixing, *Macromolecules*, 2011, **44**(15), 6094–6102.
16 F. Gubbels, R. Jerome, P. Teyssie, E. Vanlathem, R. Deltour, A. Calderone, V. Parente and J. L. Bredas, Selective localization of carbon black in immiscible polymer blends: a useful tool to design electrical conductive composites, *Macromolecules*, 1994, **27**(7), 1972–1974.
17 P. Pötschke, S. Pegel, M. Claes and D. Bonduel, A Novel Strategy to Incorporate Carbon Nanotubes into Thermoplastic Matrices, *Macromol. Rapid Commun.*, 2008, **29**(3), 244–251.
18 F. Fenouillot, P. Cassagnau and J. C. Majesté, Uneven distribution of nanoparticles in immiscible fluids: Morphology development in polymer blends, *Polymer*, 2009, **50**(6), 1333–1350.
19 S. Yang, K. Lozano, A. Lomeli, H. D. Foltz and R. Jones, Electromagnetic interference shielding effectiveness of carbon nanofiber/LCP composites, *Composites, Part A*, 2005, **36**(5), 691–697.
20 B. P. Singh, Prabha, P. Saini, T. Gupta, P. Garg, G. Kumar, I. Pande, S. Pande, R. K. Seth, S. K. Dhawan and R. B. Mathur, Designing of multiwalled carbon nanotubes reinforced low density polyethylene nanocomposites for suppression of electromagnetic radiation, *J. Nanopart. Res.*, 2011, **13**(12), 7065–7074.
21 Y. J. Kim, T. S. Shin, H. D. Choi, J. H. Kwon, Y.-C. Chung and H. G. Yoon, Electrical conductivity of chemically modified multiwalled carbon nanotube/epoxy composites, *Carbon*, 2005, **43**(1), 23–30.
22 S. B. Kharchenko, J. F. Douglas, J. Obrzut, E. A. Grulke and K. B. Migler, Flow-induced properties of nanotube-filled polymer materials, *Nat. Mater.*, 2004, **3**(8), 564–568.
23 O. Valentino, M. Sarno, N. G. Rainone, M. R. Nobile, P. Ciambelli, H. C. Neitzert and G. P. Simon, Influence of the polymer structure and nanotube concentration on the conductivity and rheological properties of polyethylene/CNT composites, *Phys. E.*, 2008, **40**(7), 2440–2445.
24 R. Reza, J. Kim and H. Naguib, Synthesis and characterization of novel low density polyethylene–multiwall carbon nanotube porous composites, *Smart Mater. Struct.*, 2009, **18**(10), 104002.
25 J. Feng and C. M. Chan, Carbon black-filled immiscible blends of poly(vinylidene fluoride) and high density polyethylene: Electrical properties and morphology, *Polym. Eng. Sci.*, 1998, **38**(10), 1649–1657.
26 P. Pötschke, A. R. Bhattacharyya and A. Janke, Morphology and electrical resistivity of melt mixed blends of polyethylene and carbon nanotube filled polycarbonate, *Polymer*, 2003, **44**(26), 8061–8069.
27 O. Koysuren, S. Yesil and G. Bayram, Effect of solid state grinding on properties of PP/PET blends and their

composites with carbon nanotubes, *J. Appl. Polym. Sci.*, 2010, **118**(5), 3041–3048.
28 S. Wu, *Polymer Interface and Adhesion*, M. Dekker, 1982.
29 S. Nuriel, L. Liu, A. H. Barber and H. D. Wagner, Direct measurement of multiwall nanotube surface tension, *Chem. Phys. Lett.*, 2005, **404**(4–6), 263–266.
30 A. H. Barber, S. R. Cohen and H. D. Wagner, Static and Dynamic Wetting Measurements of Single Carbon Nanotubes, *Phys. Rev. Lett.*, 2004, **92**(18), 186103.
31 Q. Li, S. Basavarajaiah, N. H. Kim, S.-B. Heo and J. H. Lee, Synergy effect of hybrid fillers on the positive temperature coefficient behavior of polypropylene/ultra-high molecular weight polyethylene composites, *J. Appl. Polym. Sci.*, 2010, **116**(1), 116–124.
32 J. K. Yuan, S. H. Yao, A. Sylvestre and J. Bai, Biphasic polymer blends containing carbon nanotubes: Heterogeneous nanotube distribution and its influence on the dielectric properties, *J. Phys. Chem. C*, 2012, **116**(2), 2051–2058.
33 G. D. Liang and S. C. Tjong, Electrical properties of low-density polyethylene/multiwalled carbon nanotube nanocomposites, *Mater. Chem. Phys.*, 2006, **100**(1), 132–137.
34 N. K. Shrivastava, S. Suin, S. Maiti and B. B. Khatua, Ultralow Electrical Percolation Threshold in Poly(styrene-*co*-acrylonitrile)/Carbon Nanotube Nanocomposites, *Ind. Eng. Chem. Res.*, 2013, **52**(8), 2858–2868.
35 E. Logakis, C. Pandis, V. Peoglos, P. Pissis, J. Pionteck, P. Pötschke, M. Mičušík and M. Omastová, Electrical/dielectric properties and conduction mechanism in melt processed polyamide/multi-walled carbon nanotubes composites, *Polymer*, 2009, **50**(21), 5103–5111.
36 S. Panteny, R. Stevens and C. R. Bowen, The Frequency Dependent Permittivity and AC Conductivity of Random Electrical Networks, *Ferroelectrics*, 2005, **319**(1), 199–208.
37 M. Rahaman, T. Chaki and D. Khastgir, Control of the temperature coefficient of the DC resistivity in polymer-based composites, *J. Mater. Sci.*, 2013, **48**(21), 7466–7475.
38 M. Rahaman, T. K. Chaki and D. Khastgir, Determination of Percolation Limits of Conductivity, Dielectric Constant, and EMI SE for Conducting Polymer Composites Using Sigmoidal Boltzmann Model, *J. Mater. Sci.*, 2012, **10**, 115–118.
39 B. K. Money and J. Swenson, Dynamics of Poly(ethylene oxide) around Its Melting Temperature, *Macromolecules*, 2013.
40 C. M. C. Jiyun Feng, Double positive temperature coefficient effects of carbon black-filled polymer blends containing two semicrystalline polymers, *Polymer*, 2000, **41**(12), 4559–4565.

